Antiferromagnetism and the metal-insulator transition in the infinite-dimensional Hubbard model

1995 J. Phys.: Condens. Matter 7 7335

(http://iopscience.iop.org/0953-8984/7/37/007)

J. Phys.: Condens. Matter 7 (1995) 7335–7347. Printed in the UK

Antiferromagnetism and the metal–insulator transition in the infinite-dimensional Hubbard model

S Wermbter and G Czycholl

Institut für Theoretische Physik, Universtät Bremen, Postfach 330440, D-28334 Bremen, Germany

Received 6 March 1995, in final form 11 July 1995

Abstract. We study the Hubbard model in infinite dimension $d = \infty$ within an approximation reproducing simultaneously the atomic limit and the weak-coupling limit up to second order in the interaction strength U. Depending on U we find a paramagnetic metal, a paramagnetic insulator, or an antiferromagnetic insulator. The stability of the antiferromagnetic phase is investigated by calculating the grand canonical potential. We present the phase diagram in the T–U plane and results for the magnetization m as a function of temperature T. For small values of U the antiferromagnetic phase transition is continuous, but for larger values of U the approximation yields a first-order magnetic phase transition. Results for the density of states $N(\epsilon)$ are presented; it either exhibits one single band or an upper and a lower Hubbard band separated by the Mott gap. The upper and lower Hubbard band may exhibit additional magnetic structure, depending on the value of T and U.

1. Introduction

The Hubbard model was originally introduced as the simplest model for strongly correlated electron systems which may exhibit an insulating Mott state, i.e. a metal–insulator phase transition [1, 2], and is used to model itinerant magnetism. Apart from an exact solution in one dimension for the ground state of the Hubbard model [3], no exact results are available for this problem. The main problem to deal with is the correct description of the transition from the atomic limit to the itinerant (band) limit. As regards magnetism, we know only special limits of the Hubbard model. In the limit of a small hopping parameter t compared to the interaction strength U, second-order perturbation theory with respect to the hopping t can be used to transform the Hubbard model for half filling to an effective Heisenberg model with exchange coupling $2t^2/|U|$ [4]. In this special case antiferromagnetism is predicted. Away from half filling the HM may be transformed into the t–J model [5] and antiferromagnetism should exist at least in a certain parameter regime.

Metzner and Vollhardt [6] recently introduced the limit of infinite spatial dimensionality ($d \to \infty$), in which the self-energy Σ becomes site diagonal, i.e. the local approximation becomes exact. This leads to a simplified Hubbard model for $d \to \infty$ (for a review see [7]), but the essential properties are similar as in three dimensions. Because of the simplifications one can hope to achieve the exact solution of the infinite-dimensional Hubbard model, which would provide for a proper mean-field theory of the Hubbard model in a general dimension [8, 9]. The self-energy of the infinite-dimensional Hubbard model 'knows about' the lattice only via the local propagator $G(z)$. That is why the functional dependence of the self-energy on the local Green function must be the same as in the case of an atomic problem [8, 10]

0953-8984/95/377335+13$19.50

or of an impurity problem like the single-impurity Anderson model [11]. This allows for a mapping onto an atomic problem in the presence of two time-dependent, auxiliary Kadanoff–Baym [12] fields.

For the general Hubbard model in infinite dimension only numerical methods have been possible up to now. These numerical methods have recently also been used to calculate antiferromagnetism. For example antiferromagnetism has been studied by time discretization [13], by quantum Monte Carlo calculation [14], the exact enumeration method [15], by iterated perturbation theory (IPT) [15] of the Hubbard model, and by the NCA for the effective single-impurity Anderson model [16]. In the case of a weak-coupling interaction, i.e. $U \ll t$, we know that the SCR theory of Moriya [17] or RPA-like theories [18] are successful in explaining the weakly ferromagnetic or antiferromagnetic (AF) limit.

However, because we are far away from any unified theory there exist an immense variety of approximate theories; see for instance [19] and references therein. Nevertheless, it is necessary to develop improved approximations to the infinite-dimensional Hubbard model. Improved approximations should at least reproduce the atomic limit (hopping $t = 0$), the limit of vanishing U, the weak-coupling limit and—as a result Fermi-liquid properties and with $d = \infty$—the exact solution of the Falicov–Kimball model (FKM) [20]. The Edwards–Hertz approximation (EHA) [21], the approximation of Martin-Rodero and co-workers [22], and the IPT [15] at half filling contain these limits. In this paper we investigate the magnetic properties of the EHA and the question concerning the metal–insulator transition and the antiferromagnetic–paramagnetic (AF–PM) phase transition for the symmetric case, i.e. half-filled band. For a discussion of what this model can describe see [23].

The paper is organized as follows: section 2 describes the slightly modified EHA on a bipartite AB-lattice and the basic equations; the numerical results and our discussion are presented in section 3; section 4 contains our conclusions.

2. Edwards–Hertz approximation on a bipartite AB-lattice

The Hubbard Hamiltonian reads [1]

$$H = -\frac{t^*}{\sqrt{d}} \sum_{\langle R,R'\rangle,\sigma} c^\dagger_{R,\sigma} c_{R',\sigma} + \sum_{R,\sigma} E^0_\sigma n_{R,\sigma} + U \sum_R n_{R,\uparrow} n_{R,\downarrow} \tag{1}$$

where $c^\dagger_{R,\sigma}$ ($c_{R,\sigma}$) creates (annihilates) an electron at site R of the d-dimensional hypercubic lattice and $n_{R,\sigma} = c^\dagger_{R,\sigma} c_{R,\sigma}$. σ is the spin index and E^0_σ denotes the bare atomic energy for spin-up, spin-down electrons, t is the nearest-neighbour hopping matrix element and U is the on-site Coulomb interaction strength. The hopping term in the Hamiltonian is restricted to nearest neighbours. The scaling of the hopping term provides for a non-trivial limit in infinite dimension $d = \infty$ [6, 7]. The density of states $N^0(\epsilon)$ per spin direction of the non-interacting system has a Gaussian form [6]:

$$N^0(\epsilon) = \frac{1}{t^*\sqrt{\pi}} \exp\left(-\left(\epsilon/t^*\right)^2\right) \tag{2}$$

with $4t^2 d = t^{*2} = \text{constant}$. The on-site self-energy $\Sigma_\sigma(R, R; \mathrm{i}\omega_n)$ of a bipartite AB-lattice, can be written as follows:

$$\Sigma_\sigma(R, R; \mathrm{i}\omega_n) = \Sigma_{1,\sigma}(\mathrm{i}\omega_n) + \Sigma_{2,\sigma}(\mathrm{i}\omega_n) \mathrm{e}^{\mathrm{i}Q\cdot R} = \begin{cases} \Sigma_{A,\sigma}(\mathrm{i}\omega_n) & \text{for } R \in \text{lattice } A \\ \Sigma_{B,\sigma}(\mathrm{i}\omega_n) & \text{for } R \in \text{lattice } B. \end{cases} \tag{3}$$

For an AF ordered state we have $Q = (\pi, \pi, ...)$ and the following symmetry of the self-energy:

$$\Sigma_{A,\sigma} = \Sigma_{B,-\sigma}. \tag{4}$$

We set the lattice constant a to unity. For a ferromagnetic or PM state we have the symmetry $\Sigma_{A,\sigma} = \Sigma_{B,\sigma}$.

We restrict the calculation to the sublattice A and drop the index A. After inverting the Dyson equation $G^{-1} = G^{0^{-1}} - \Sigma$, we get the local Green function

$$G_\sigma(i\omega_n) = \frac{i\omega_n + \mu - \Sigma_1(i\omega_n) + \sigma\Sigma_2(i\omega_n)}{\sqrt{[i\omega_n + \mu - \Sigma_1(i\omega_n)]^2 - \Sigma_2(i\omega_n)^2}} \int_{-\infty}^{\infty} d\epsilon\ N^0(\epsilon) \times \frac{1}{\sqrt{[i\omega_n + \mu - \Sigma_1(i\omega_n)]^2 - \Sigma_2(i\omega_n)^2 - \epsilon}} \tag{5}$$

with the definitions

$$\Sigma_1(i\omega_n) = \frac{1}{2}[\Sigma_\uparrow(i\omega_n) + \Sigma_\downarrow(i\omega_n)] \qquad \Sigma_2(i\omega_n) = \frac{1}{2}[\Sigma_\uparrow(i\omega_n) - \Sigma_\downarrow(i\omega_n)] \tag{6}$$

and $\sigma = +1$ (-1) for electrons with spin $\uparrow$ $(\downarrow)$. μ is the chemical potential. The fermion Matsubara frequency is defined by $\omega_n = (2n+1)\pi/\beta$, $n = 0, \pm1, \pm2, ...,$ and $\beta = 1/k_BT$. For the PM state, Σ_2 is zero and equation (5) reduces to the standard expression for the on-site Green function in infinite dimension. The occupation number of the spin-σ electrons of the interacting system is defined by

$$n_\sigma = \lim_{\tau \to +0} \frac{1}{\beta} \sum_n e^{i\omega_n \tau} G_\sigma(i\omega_n) = \frac{1}{2} + \frac{2}{\beta} \sum_{n=0}^{\infty} \mathrm{Re}\, G_\sigma(i\omega_n). \tag{7}$$

We define the magnetization on the sublattice as

$$m = \frac{1}{2}(n_\uparrow - n_\downarrow). \tag{8}$$

Recall that because we restricted ourselves to sublattice A, the magnetization for sublattice B is given by $m_B = -m$.

According to Edwards and Hertz [21] we use the following *ansatz* for the self-energy on the imaginary axis:

$$\Sigma_\sigma(i\omega_n) = \frac{U n_{-\sigma}}{1 - (U - \Sigma_\sigma(i\omega_n))\tilde{G}^0_\sigma(i\omega_n - \Sigma_\sigma + E_\sigma)} \tag{9}$$

where

$$\tilde{G}^0_\sigma(\tau) = -\frac{G^{HF}_\sigma(\tau) G^{HF}_{-\sigma}(\tau) G^{HF}_{-\sigma}(-\tau)}{n_{-\sigma}(1 - n_{-\sigma})}. \tag{10}$$

The Matsubara Green function $G(i\omega_n)$ is the Fourier coefficient of the periodic temperature Green function $G_\sigma(\tau)$:

$$G_\sigma(\tau) = \frac{1}{\beta} \sum_n e^{-i\omega_n \tau} G_\sigma(i\omega_n) \qquad G_\sigma(i\omega_n) = \int_0^\beta e^{i\omega_n \tau} G_\sigma(\tau)\, d\tau. \tag{11}$$

With the help of equations (11) we get for the approximation for $\tilde{G}^0(z)$ (equation (10))

$$\tilde{G}^0_\sigma(i\omega_n - \Sigma_\sigma + E_\sigma) = -\frac{1}{n_{-\sigma}(1 - n_{-\sigma})} \int_0^\beta d\tau\ e^{i\omega_n \tau} \left\{ G^{HF}_{-\sigma}(\tau) G^{HF}_{-\sigma}(-\tau) \times \frac{1}{\beta} \sum_n e^{-i\omega_n \tau} G^{HF}_\sigma(i\omega_n - \Sigma_\sigma + E_\sigma) \right\}. \tag{12}$$

Note that the band filling $n_{-\sigma}$ is the filling of the system described by the *ansatz* for the self-energy (equation (9)). G^{HF} in equation (10) and equation (12) is the Hartree–Fock Green function, i.e. it is determined by equations (5), (11) with the replacement

$$\Sigma_1(\mathrm{i}\omega_n) = \frac{1}{2}(E_\uparrow + E_\downarrow) \qquad \Sigma_2(\mathrm{i}\omega_n) = \frac{1}{2}(E_\uparrow - E_\downarrow). \tag{13}$$

For this case the self-energies Σ_1, Σ_2 are independent of frequency.

The effective atomic levels E_σ for introduced the σ-electrons have to be determined self-consistently under the constraint

$$E_\uparrow + E_\downarrow = Un. \tag{14}$$

n is the full occupation number: $n = n_\uparrow + n_\downarrow$ and for half filling $n = 1$ the self-consistent calculation of the effective atomic levels reduces to the relation

$$E_\sigma = Un_{-\sigma}. \tag{15}$$

The approximation (10) for $\tilde{G}^0_\sigma(\tau)$ reproduces the second-order perturbation theory (SOPT), when expanding the self-energy expression (9) in powers of the Coulomb correlation U up to second order in U and the atomic limit; also the exact Brandt–Mielsch solution [10] of the FKM [20] is contained in the general approximation (9).

For half filling we have the chemical potential $\mu = U/2$. In this case the true occupation number n, corresponding to the Green functions G_σ to be determined, is equal to the occupation number $\tilde{n}^0$, corresponding to $\tilde{G}^0_\sigma$:

$$\tilde{n}^0_\sigma = \tilde{n}^0_\uparrow + \tilde{n}^0_\downarrow = 1 + \frac{2}{\beta}\sum_{n=0}^{\infty}\left(\mathrm{Re}\,\tilde{G}^0_\uparrow(\mathrm{i}\omega_n) + \mathrm{Re}\,\tilde{G}^0_\downarrow(\mathrm{i}\omega_n)\right).$$

If we are away from half filling, we have to calculate the chemical potential self-consistently, until the constraint $n = \tilde{n}^0 = \tilde{n}^0_\sigma + \tilde{n}^0_{-\sigma}$ is fulfilled.

Nevertheless, in both cases we have to calculate self-consistently the effective atomic levels and the band fillings $n_\uparrow, n_\downarrow$ under the constraint $n_\uparrow + n_\downarrow = 1$.

To obtain information on the thermodynamically stable phase we must calculate the grand canonical potential (GCP). The GCP is determined by a coupling constant integration:

$$\Delta\Omega_U = \int_0^1 \frac{\mathrm{d}\lambda}{\lambda}\Delta\Omega_\lambda$$

$$\Delta\Omega_{(\lambda=U_{eff}/U)} = \lim_{\eta\to 0^+}\frac{1}{2}\frac{1}{\beta}\sum_{\omega_n} \mathrm{e}^{\mathrm{i}\omega_n\eta}\left[\Sigma_1^{(\lambda)}(\mathrm{i}\omega_n)\{G_\uparrow^{(\lambda)}(\mathrm{i}\omega_n) + G_\downarrow^{(\lambda)}(\mathrm{i}\omega_n)\}\right.$$
$$\left. + \Sigma_2^{(\lambda)}(\mathrm{i}\omega_n)\{G_\uparrow^{(\lambda)}(\mathrm{i}\omega_n) - G_\downarrow^{(\lambda)}(\mathrm{i}\omega_n)\}\right]. \tag{16}$$

$\Delta\Omega_U$ is the difference between the GCP of the actual system and that of the system without interaction ($U = 0$). $\Sigma_\sigma^{(\lambda)}$ and $G_\sigma^{(\lambda)}$ are the self-energy and the Green function for the effective interaction strength $U_{eff} = \lambda U$. For fixed temperature T there exists a lower bound of the coupling constant λ_c, at which no AF phase exists. The corresponding interaction strength is $U_{eff} = U\lambda_c$. It follows that

$$\Delta\Omega^{AF} - \Delta\Omega^{PARA} = \lim_{\eta\to 0^+}\frac{1}{2}\int_{\lambda_c}^1 \frac{\mathrm{d}\lambda}{\lambda}\left\{\Delta\Omega_\lambda^{AF} - \Delta\Omega_\lambda^{PARA}\right\} \tag{17}$$

with $T_c^{(\lambda_c)} = T$, where $\Delta\Omega^{AF}$ denotes the GCP in the AF phase and $\Delta\Omega^{PARA}$ denotes the GCP in the PM phase ($n_\uparrow = n_\downarrow$). To calculate the GCP in the PM phase we start with $n_\uparrow = n_\downarrow = 0.5$, which is always a solution of the equations.

Having obtained the thermodynamic information of the system, we have to calculate the density of states $N(\omega)$. Recently we calculated the density of states for the PM case [23]. With the help of equations (3)–(11) in [23] we are able to calculate the density of states for the AF case. Because we are now looking for solutions on the real axis, we solve the problem with the help of the Kramers–Kronig relation. The approximation (10) takes the form

$$\tilde{G}_\sigma(z) = \int_{-\infty}^{\infty} d\omega' \, \frac{\tilde{N}_\sigma^0(\omega')}{z - \Sigma_\sigma(z) + E_\sigma - \omega'} \tag{18}$$

$$\begin{aligned}\tilde{N}_\sigma^0(\omega) = \frac{1}{n_{-\sigma}(1-n_{-\sigma})} \int_{-\infty}^{\infty}\int_{-\infty}^{\infty}\int_{-\infty}^{\infty} d\omega_1 \, d\omega_2 \, d\omega_3 \; N_{-\sigma}^0(\omega_1) N_{-\sigma}^0(\omega_2) \\ \times N_\sigma^0(\omega_3)\{f(\omega_1)[1-f(\omega_2)] \\ + f(\omega_3)[f(\omega_2) - f(\omega_1)]\}\, \delta(\omega + \omega_1 - \omega_2 - \omega_3).\end{aligned} \tag{19}$$

In equation (9) the Matsubara frequency is replaced by $z \to \omega + i0^+$ and $\tilde{G}_\sigma^0(i\omega_n - \Sigma_\sigma + E_\sigma)$ by $\tilde{G}_\sigma(z)$. The unperturbed bipartite AB density of states N_σ^0 has the form

$$N_\sigma^0(\omega) = \begin{cases} 0 & \text{for } |\omega - E_1| \leqslant |E_2| \\ \left[(\omega - E_1 + \sigma E_2)/\sqrt{[\omega - E_1]^2 - E_2^2}\right] N^0 & \\ \times \left(\sqrt{[\omega - E_1]^2 - E_2^2}\right) \operatorname{sign}(\omega - E_1) & \text{otherwise} \end{cases} \tag{20}$$

with

$$E_1 = \frac{1}{2}(E_\uparrow + E_\downarrow) \qquad E_2 = \frac{1}{2}(E_\uparrow - E_\downarrow) \tag{21}$$

and $\operatorname{sign}(x) = 1$ for $x \geqslant 0$, $\operatorname{sign}(x) = -1$ for $x \leqslant 0$.

The equations are solved for given U, and T, and total occupation number $n = n_\sigma + n_{-\sigma}$. We start from an initial guess for the band fillings $n_\sigma, n_{-\sigma}$ and chemical potential μ, and determine the effective atomic levels E_σ necessary to yield the given n_σ. In the special case of half filling ($n = 1$) certain simplifications hold, namely for symmetric reasons we have $\mu = U/2$ and $E_\sigma = Un_{-\sigma}$. With the help of these effective levels, we are able to solve the CPA-like equation (9) for the self-energy. Knowledge of the self-energy allows us to calculate the Matsubara Green function (equation (5)) and the band fillings. The resulting band filling allows for a new determination of the effective levels E_σ and the procedure is iterated until convergence is reached. Away from half filling a further self-consistency has to be added, i.e. the full occupation number allows for a new determination of the chemical potential μ so that the guessed band filling is reproduced and the procedure is iterated until convergence is reached. Numerical results are presented in the following section.

3. Numerical results and discussion

For our numerical calculations we measure energies, frequencies and temperature in units of the effective bandwidth $t^* = 1$. We restrict the calculation to the half-filled system. At half filling the chemical potential is $\mu = U/2$ and the effective atomic levels are $E_\sigma = Un_{-\sigma}$.

Figure 1(a) shows the Neél temperature T_c determined as the lowest temperature at which the magnetization m vanishes, as a function of the interaction strength U for a self-consistent Hartree–Fock (HF) approximation, a self-consistent SOPT approximation relative to the Hartree term (SOPT-HF) and for the EHA approximation. For all three calculations

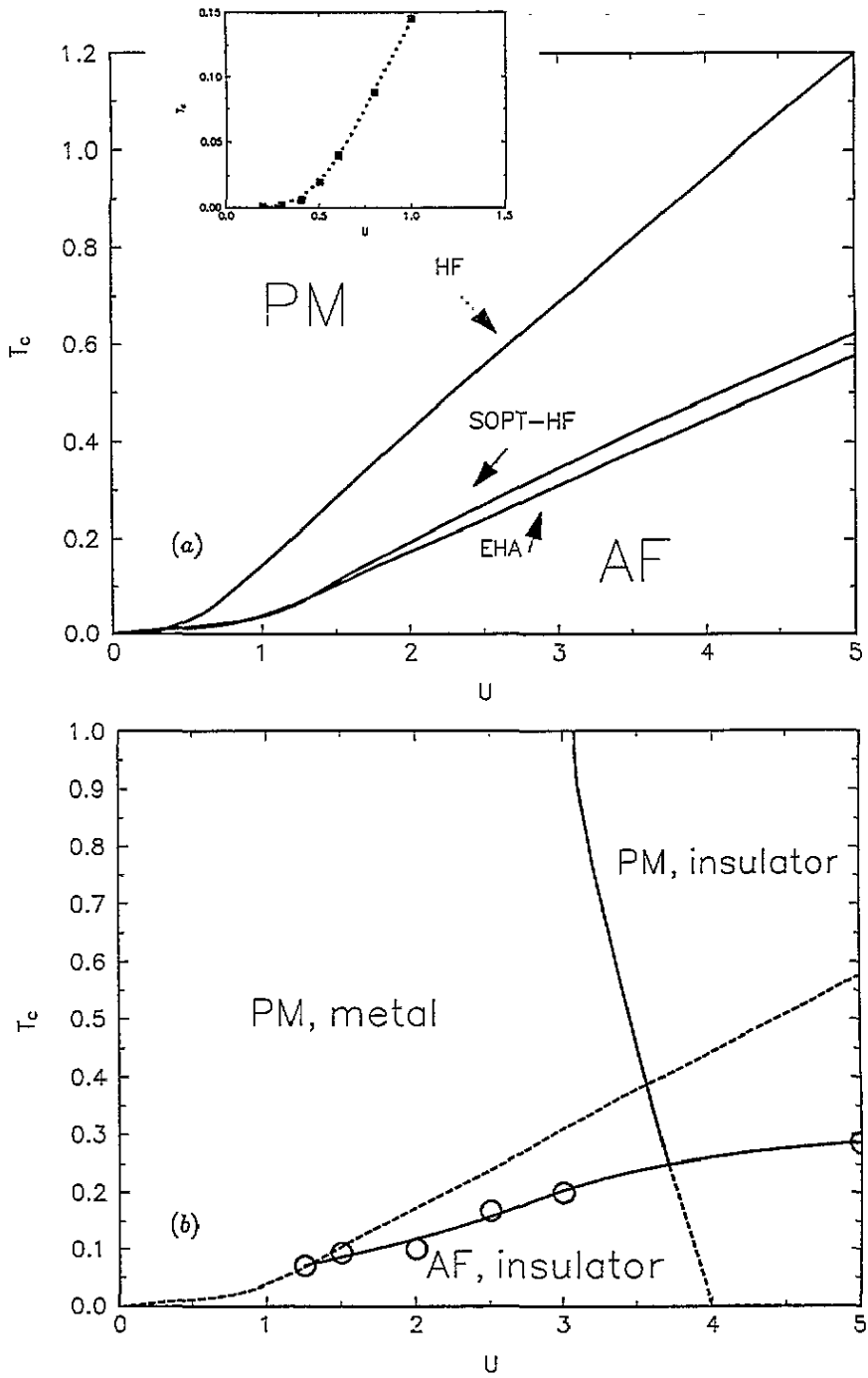

Figure 1. (a) Neél temperature T_c calculated from magnetization as a function of U, for band filling $n = 1$ and chemical potential $\mu = U/2$ obtained within the self-consistent HF, SOPT-HF, and EHA calculations. Inset: Neél temperature T_c as a function of U for the self-consistent HF calculation. (b) Thermodynamic stable phase diagram in the T–U plane determined as the phase with the lowest GCP, band filling $n = 1$ and chemical potential $\mu = U/2$. The dashed line indicates the phase transition as obtained within the EHA without calculating the GCP.

the Neél temperature T_c increases with increasing interaction strength U and no saturation or decrease of the Neél temperature T_c is observed. For small interaction strength (roughly $U \leqslant 1$) the Neél temperature T_c determined within the SOPT-HF coincides with that obtained within the EHA. Also no saturation or decrease of T_c as a function of increasing U is observed in a fully self-consistent SOPT calculation [24]. For small U it follows from SOPT calculations [24] that $T_c \sim b\exp(-a/U)$, which is also correct for the simple self-consistent Hartree calculation (see the inset of figure 1(a)). However, the calculation shows that roughly for $U \geqslant 1$ a first-order transition occurs and with increasing U the Neél temperature increases. Hence we obtain an unusual kind of magnetism in the EHA model, at least for $U \geqslant 1$. A similar result has been obtained in SOPT [24], within which for small interaction strength ($U \leqslant 1.4$) a continuous magnetic phase transition occurs, but for larger values of U a first-order transition occurs. However, we cannot exclude the possibility that the first-order transition might be an artifact of the approximation made for intermediate coupling strength U. On the other hand, we do not know of any principle or argument excluding first-order AF phase transitions.

As we can see from figure 1(a) SOPT and the EHA yield a substantial correction for the original Neél temperature compared to the corresponding result obtained within the Hartree approximation, but there is only a small difference between the Neél temperature for the SOPT calculation compared to that for the EHA calculation. We conclude that the metal–insulator transition in the EHA model has only a small effect on the Neél temperature, because in the EHA the metal–insulator transition is present, but in SOPT it is absent. Enumeration methods [15] and the NCA [16] do not support the existence of a magnetic first-order transition.

In figure 1(b) we present the thermodynamic stable phase diagram for the EHA in the T–U plane. We observe three stable phases, a PM metal, a PM insulator and an AF insulator. For interaction strength $U \leqslant 3$ we observe a PM metal and an AF insulator, which survives for very small interaction strength U only at zero temperature. For larger U the system may come into the PM insulating phase, which first occurs as a function of temperature roughly for $T \geqslant 0.25$ and $U \geqslant 3.75$. Below this temperature the system is an AF insulator. If we artificially extend the PM metal–insulator transition into the AF phase we get the dashed line in figure 1(b). In the PM phase we obtain a continuous phase transition between the insulating phase and the metallic phase, but a first-order magnetic phase transition at least for $U \geqslant 1$.

The dashed line in the PM region corresponds to the 'EHA line' of figure 1(a), i.e. it indicates the phase transition between the PM phase and the AF phase as obtained within the EHA without calculating the GCP. For intermediate values of U ($U \geqslant 2$) one would obtain an additional phase, an AF metal, which develops as a function of U between the AF insulator and the PM metal/PM insulator. However, the calculation of the GCP shows that it is not sufficient to calculate the Neél temperature as the lowest temperature at which the magnetization m vanishes and that the AF metallic phase is not stable. Furthermore the GCP shows that the EHA yields a first-order magnetic phase transition for $U \geqslant 1$ but for $U \leqslant 1$ a second-order magnetic phase transition, and that three thermodynamic stable phases occur: a PM metal, a PM insulator and an AF insulator. The calculated Neél temperature has no local maximum in the regime from $U = 0$ to $U = 5$ and it reaches the value of 0.28 for $U = 5$, which is twice as large as the value obtained using IPT [15] or QMC methods [14] for $U \simeq 3$. As in the calculation without the GCP the Neél temperature does not decrease as the interaction strength U is increased but saturates at least for $U \leqslant 5$.

IPT [15] gives a different picture; a second-order magnetic phase transition and a first-order transition between the PM metal and the Mott PM insulator, i.e. a region with two

different solutions (metal and insulator), has been obtained. The corresponding interaction strengths are $U_{c1} \simeq 3.7$, $U_{c2} \simeq 4.5$ for $T = 0$ K, which are of the same magnitude as for our transition temperature. IPT gives a maximum in the Neél temperature for interaction strength $U \simeq 3$ and it never exceeds the value $T_c \simeq 0.14$. Nearly the same values were reported from QMC studies [14]. These results are different from the EHA results, because in the EHA the Neél temperature never decreases as the interaction strength U is increased. The reason for this behaviour is that EHA is not correct up to second order in the hopping matrix element t, i.e. the limit in which the Hubbard model becomes equivalent to the t–J model is not properly reproduced in the EHA.

Figure 2(a) presents the result for the magnetization m as a function of temperature T for different interaction strengths U. In the inset of the figure we show the magnetization as a function of temperature for the HF calculation and the SOPT-HF calculation. For roughly $U \leqslant 1$, the EHA and SOPT-HF calculation show a continuous AF phase transition, but with increasing U a change to a first-order transition is observed. The same happens in fully self-consistent SOPT [24]. As there has been up to now no experimental indication for a first-order magnetic phase transition, one has to be sceptical and should stress that this finding may be an artifact of the approximations. Including the results of the calculation of the GCP, the magnetization curves are cut at the temperature $k_BT \simeq 0.1, 0.125$ for $U = 2, 2.5$ yielding a first-order transition too.

In figure 2(b) we show the result for the magnetization m as a function of interaction strength U for different temperatures T. As before, the magnetization m as a function of U never decreases as U is increased, at least for $U \leqslant 5$. The magnetization saturates for increasing U approximating the value of 0.5. This is not the correct physical picture, because for half filling and $U \gg t$ we can transform the Hubbard model to an effective Heisenberg model with exchange coupling $J = 2t^2/|U|$. In a simple molecular field treatment of the Heisenberg model the Neél temperature is proportional to the exchange coupling constant J, which is why T_c and the magnetization should asymptotically go to zero as U is increased.

In figure 3(a) we present the AF density of states $N_\sigma(\omega)$ for different values of temperature T as a function of energy ω for interaction strength $U = 2$. We see the AF gap roughly for $T \leqslant 0.15$; the system is an AF insulator. For higher temperatures the AF gap reduces to a pseudogap and the system becomes a thermodynamically unstable AF metal, which goes into the PM phase for $T = 0.1722$. This behaviour of the system is demonstrated in the inset. For temperature $k_BT = 0.15$ the density of states shows an AF gap between the lower and upper Hubbard bands. For half filling we have an AF insulator. Increasing the temperature to 0.16 the AF gap vanishes to a pseudogap and the density of states shows only one partially filled single band; consequently the system is an AF metal. The sum rule is fulfilled. The upper and lower Hubbard bands show additional structure due to the sublattice structure of the antiferromagnet. The densities of states $N_\uparrow$, $N_\downarrow$ are symmetric around the chemical potential for half filling (see figure 3(b)). The additional magnetic structure in the subbands is well understood in the Stoner picture for band antiferromagnetism. In the Stoner model the subbands are rigidly shifted with respect to each other by an energy of Um [19]

In figures 4(a) and 4(b) we show our results for the imaginary part and the real part of the self-energy for interaction strength $U = 2$ as a function of frequency for different temperatures T. The imaginary part of the self-energy shows the AF gap and the additional structure due to the sublattice structure.

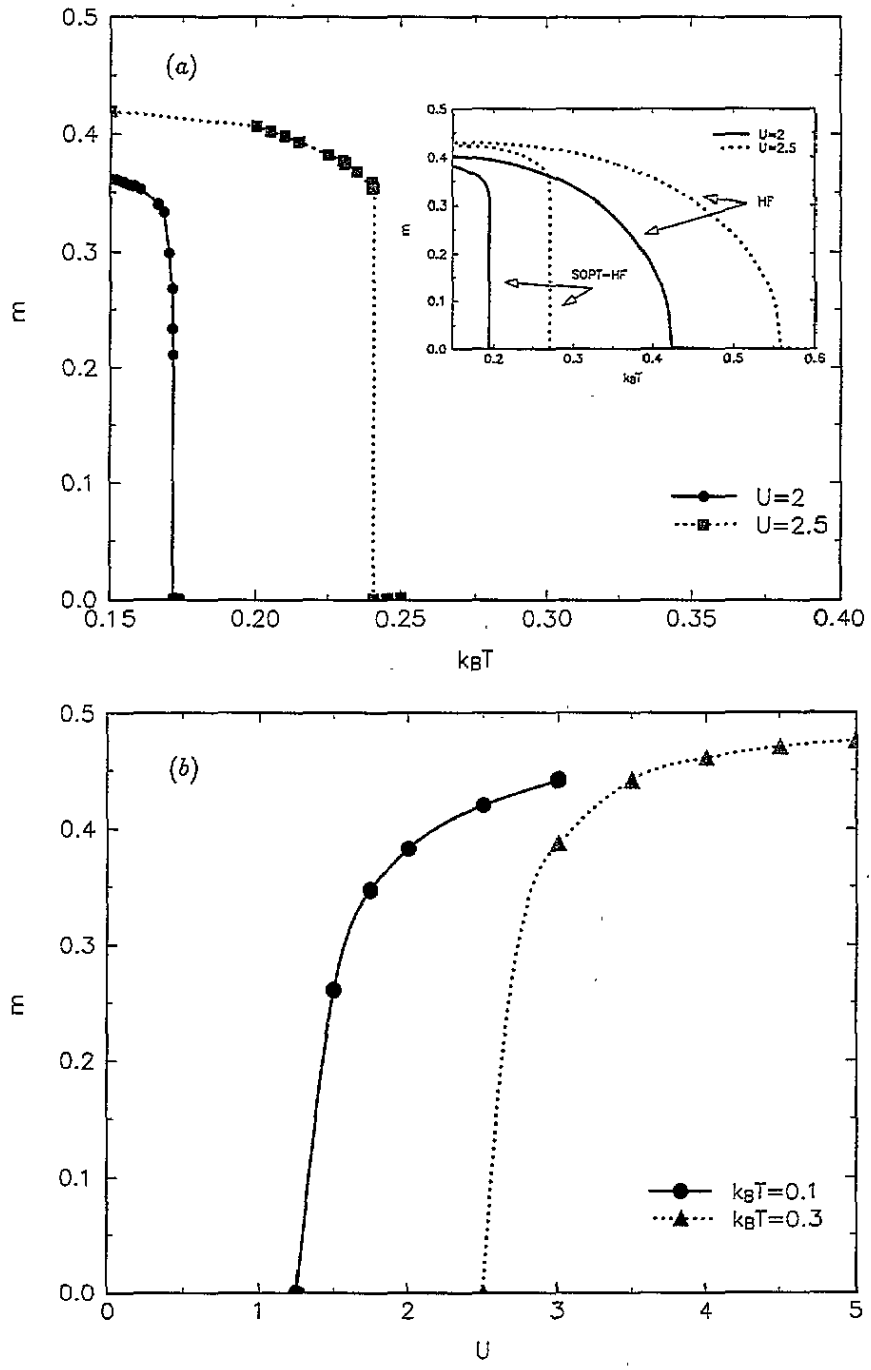

Figure 2. (a) Magnetization m as a function of temperature k_BT for interaction strength $U = 2$ and $U = 2.5$, band filling $n = 1$ and chemical potential $\mu = U/2$. Inset: m as a function of k_BT for HF, and SOPT-HF calculations. (b) Magnetization m as a function of U for temperatures $k_BT = 0.1, 0.3$, band filling $n = 1$ and chemical potential $\mu = U/2$.

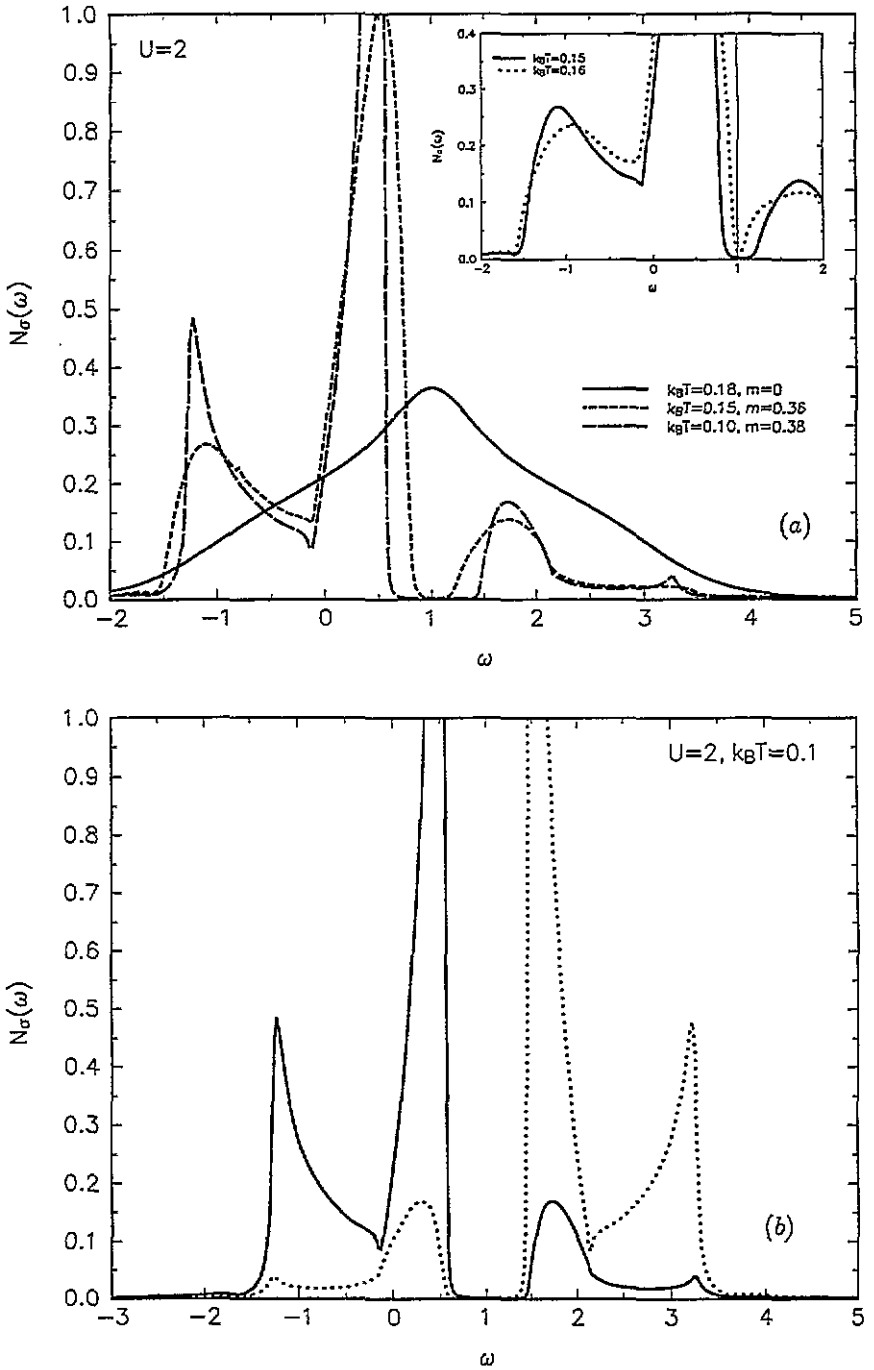

Figure 3. (a) Density of states $N_\sigma(\omega)$ as a function of energy ω for different values of k_BT for $U = 2$, band filling $n = 1$ and chemical potential $\mu = U/2$. Inset: density of states for $k_BT = 0.15, 0.16$ for $U = 2$. (b) Density of states $N_\sigma(\omega)$ as a function of energy ω for $k_BT = 0.1$ and $U = 2$, band filling $n = 1$ and chemical potential $\mu = U/2$. The solid curve corresponds to $N_\uparrow(\omega)$, the dotted line to $N_\downarrow(\omega)$.

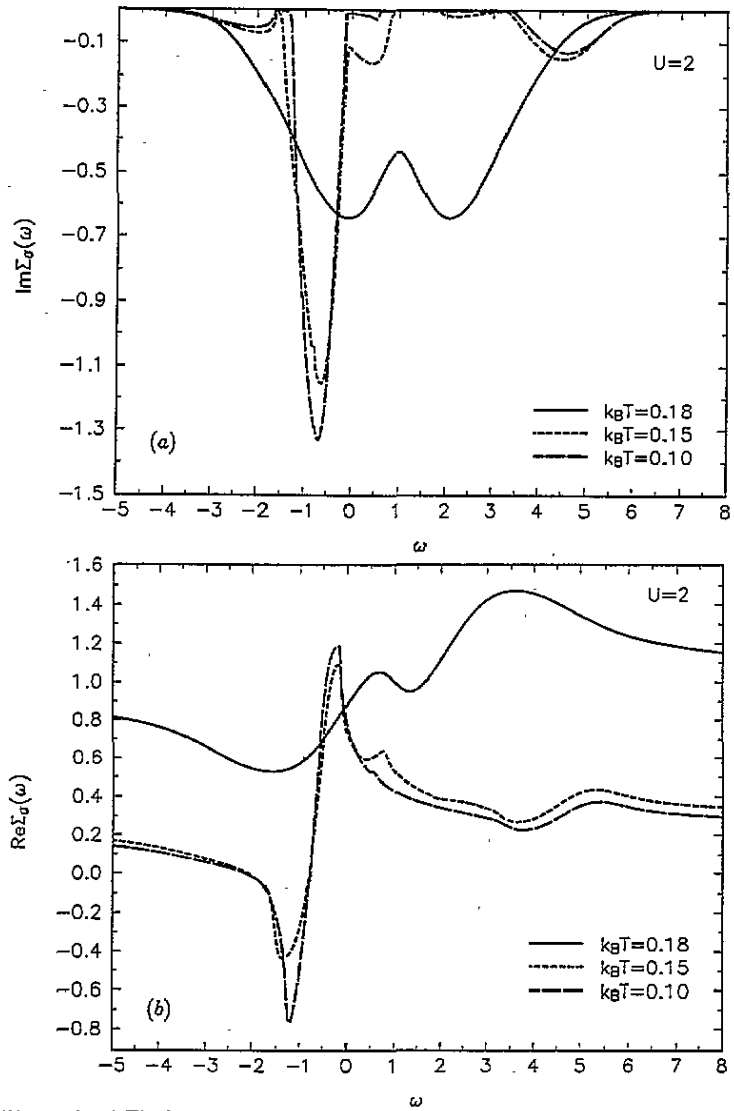

Figure 4. (a) The imaginary part of the self-energy $\Sigma(\omega)$ as a function of ω for different values of k_BT and interaction strength $U = 2$, band filling $n = 1$ and chemical potential $\mu = U/2$. (b) The real part of the self-energy $\Sigma(\omega)$ as a function of ω for different values of k_BT and interaction strength $U = 2$, band filling $n = 1$ and chemical potential $\mu = U/2$.

4. Conclusions

In the present paper we investigate the possibility of antiferromagnetism and of a metal–insulator transition in the EHA for the $d \to \infty$ Hubbard model at half filling. From the earlier papers [21, 23] we know that the EHA is exact in the atomic limit, i.e. in the limit of vanishing hopping t, but not to order t^2, which should reproduce the Heisenberg limit, and exact in the band limit. In the weak-coupling limit the EHA can be expanded in the interaction strength and agrees up to second order with the standard expressions for the self-energy. Furthermore the EHA is exact for the $d = \infty$ FKM.

The EHA is applicable for small interaction strength U and contains SOPT Fermi-liquid properties. Since the EHA is constructed to recover the above limits and is of interpolating type, it contains a metal–insulator transition as the Hubbard III or alloy analogue approximation [2].

Despite the fact that we know that the local approximation for the self-energy is exact in infinite dimension, we do not know the functional dependence of the self-energy on the local Green function. Having used a diagrammatic analysis [25] of the electron self-energy in the local approximation Edwards obtained the self-energy functional: $\Sigma = S_1[G/(1+\Sigma G)]$ and $S_1[G]$ is universal for $d = \infty$. Using this diagrammatic analysis we could recover the EHA. There S_1 was the alloy analogy functional with G replaced by $\tilde{G}$ (for details see [25]). However, the main justification for the EHA is the correct weak-coupling limit and the exact atomic limit (vanishing hopping). This confirms reliability of the EHA, i.e. we think that in the weak-coupling case the EHA can be justified; then Fermi-liquid behaviour occurs (for half filling in the paramagnetic case and $T = 0$ for $U \leqslant 2$).

The EHA contains three thermodynamic stable phases: a PM metallic phase, a PM insulating phase and an AF insulating phase. For interaction strength $U \geqslant 1$ the model shows a first-order magnetic phase transition. Below this interaction strength the EHA shows the normally expected second-order transition. The Neél temperature as a function of U does not have the right asymptotic behaviour, i.e. it never goes to zero as U is increased.

An advantage of the EHA is the fact that it is able to deal with all temperatures and with imaginary and real frequencies and, judged from the reproduction of exactly known limits, the EHA appears to be one of the best existing general approximation schemes of the Hubbard model, at least for infinite dimension.

Nevertheless, the EHA contains several difficulties. First of all the EHA does not contain the t–J limit for $U \gg t$ and as a consequence does not give the right behaviour of the Neél temperature, $T_c \sim t^2/|U|$. The EHA contains for intermediate coupling strength U a metallic non-Fermi-liquid phase and a first-order AF transition, which has never been observed. In particular these results obtained for intermediate U may be regarded as an artifact of the EHA.

In conclusion we can say that the EHA is not completely satisfactory, in the sense that the EHA should be corrected to include the self-energy contributions in order t^2 and if possible in further powers in U.

References

[1] Hubbard J 1963 *Proc. R. Soc.* A **276** 238
[2] Hubbard J 1964 *Proc. R. Soc.* A **281** 401
[3] Lieb E H and Wu F Y 1968 *Phys. Rev. Lett.* **20** 1445
[4] Anderson P W 1963 *Solid State Physics* vol 14 (New York: Academic) p 99
[5] Gros C, Joynt R and Rice T M 1987 *Phys. Rev.* B **36** 8190
[6] Metzner W and Vollhardt D 1989 *Phys. Rev. Lett.* **62** 324
[7] Vollhardt D 1993 *Correlated Electron Systems* ed V J Emery (Singapore: World Scientific) p 57
[8] Janis V 1991 *Z. Phys.* B **83** 227; 1989 *Phys. Rev.* B **40** 11331
[9] Janis V and Vollhardt D 1992 *Int. J. Mod. Phys.* **6** 731
[10] Brandt U and Mielsch C 1989 *Z. Phys.* B **75** 365; 1990 *Z. Phys.* B **79** 295; 1991 *Z. Phys.* B **82** 37
[11] Georges A and Kotliar G 1992 *Phys. Rev.* B **45** 6479
[12] Baym G and Kadanoff L P 1961 *Phys. Rev.* **124** 287
Baym G 1962 *Phys. Rev.* **127** 1391
[13] Giesekus A and Brandt U 1993 *Phys. Rev.* B **48** 10311
[14] Jarrell M 1992 *Phys. Rev. Lett.* **69** 168

Jarrell M and Pruschke Th 1993 *Z. Phys.* B **90** 187
[15] Georges A and Krauth W 1993 *Phys. Rev.* B **48** 7167
[16] Hülsenbeck G and Stephan F 1994 *Z. Phys.* B **94** 281
[17] Moriya T 1985 *Spin Fluctuations in Itinerant Electron Magnetism (Springer Series in Solid-State Sciences)* (Berlin: Springer)
[18] Brandt U, Pesch W and Tewordt L 1970 *Z. Phys.* **238** 121
Brandt U, Lustfeld H, Pesch W and Tewordt L 1971 *J. Low Temp. Phys.* **4** 79
[19] Nolting W and Borgiel W 1989 *Phys. Rev.* B **39** 6962
[20] Falicov L M and Kimball J C 1969 *Phys. Rev. Lett.* **22** 997
[21] Edwards D M and Hertz J A 1990 *Physica* B **163** 527
[22] Martin-Rodero A, Louis E, Flores F and Tejedor C 1986 *Phys. Rev.* B **33** 1814
[23] Wermbter S and Czycholl G 1994 *J. Phys.: Condens. Matter* **6** 5439
[24] Halvorsen E and Czycholl G 1994 *J. Phys.: Condens. Matter* **6** 10331
[25] Edwards D M 1993 *J. Phys.: Condens. Matter* **5** 161